Available online at www.sciencedirect.com

SciVerse ScienceDirect

Ceramics International 38 (2012) 1249–1254

CERAMICS
INTERNATIONAL

www.elsevier.com/locate/ceramint

Effects of Sb content on electrical properties of lead-free piezoelectric $(K_{0.4425}Na_{0.52}Li_{0.0375})$ $(Nb_{0.9625-x}Sb_xTa_{0.0375})O_3$ ceramics

Xuming Pang, Jinhao Qiu *, Kongjun Zhu, Yang Cao

State Key Laboratory of Mechanics and Control of Mechanical Structures, Nanjing University of Aeronautics and Astronautics, Nanjing 210016, PR China

Received 21 July 2011; received in revised form 28 August 2011; accepted 29 August 2011
Available online 3 September 2011

Abstract

Lead-free $(K_{0.4425}Na_{0.52}Li_{0.0375})$ $(Nb_{0.9625-x}Sb_xTa_{0.0375})O_3$ piezoelectric ceramics were prepared by the conventional sintering method. The effects of the Sb content on the phase structure, microstructure, dielectric, piezoelectric, and ferroelectric properties of the $(K_{0.4425}Na_{0.52}Li_{0.0375})$ $(Nb_{0.9625-x}Sb_xTa_{0.0375})O_3$ ceramics were investigated. The much higher Pauling electronegativity of Sb compared with Nb makes the ceramics more covalent. By increasing x from 0.05 to 0.09, all samples exhibit a single perovskite structure with an orthorhombic phase over the whole compositional range, and the bands in the Raman scattering spectra shifted to lower frequency numbers. The grain growth of the ceramics was improved by substituting Sb^{5+} for Nb^{5+}. Significantly, the $(K_{0.4425}Na_{0.52}Li_{0.0375})$ $(Nb_{0.8925}Sb_{0.07}Ta_{0.0375})O_3$ ceramics show the peak values of the piezoelectric coefficient (d_{33}), electromechanical coupling coefficient (k_p), and dielectric constant (ε), which are 304 pC/N, 48% and 1909, respectively, owing to the densest microstructure of typical bimodal grain size distributions. Besides, the underlying mechanism for variations of the electrical properties due to Sb^{5+} substitution was explained in this work.

Keywords: Dielectric properties; Piezoelectric properties; Sintering

1. Introduction

Lead zirconate titanate (PZT) and PZT-based piezoelectric ceramics possess excellent electrical properties and hence have been widely used in piezoelectric buzzers, transformers, sensors, and microelectronic devices. However, the high toxicity of lead oxide has caused serious environmental problems. The rapid development of piezoelectric devices urgently calls for environmental-friendly materials as substitution of the widely used lead-based ceramics. Recently, Saito et al. [1] reported that a high d_{33} (~416 pC/N) constant was obtained in the textured $(K_{0.5}Na_{0.5})NbO_3$-based ceramics near the composition of the morphotropic phase boundary (MPB). However, for pure $(K_{0.5}Na_{0.5})NbO_3$ (KNN) system prepared by normal sintering, the highest piezoelectric coefficient was about 80pC/N [2–6]. In order to improve the sintering performance and electrical properties of KNN ceramics, much research work have been carried out, including the application of various fabricating techniques such as spark-plasma sintering and hot pressing [7,8], and doping elements into the KNN ceramics have been made [2,9–12]. The results show that ion substitution plays an important role in the improvement of density and on the electrical properties of KNN-based ceramics. A recent study shows that using Sb^{5+} to substitute for Nb^{5+} in the $(K_{0.5}Na_{0.5})_{0.945}Li_{0.055}NbO_3$ ceramics can significantly improve the density and piezoelectric performance of the ceramics [13]. However, there is few report on the effects of Sb^{5+} on the properties of the (K, Na, Li) (Nb, Ta)O_3 system although the (K, Na, Li) (Nb, Ta, Sb)O_3 system show the excellent properties [1]. In this work, all the $(K_{0.4425}Na_{0.52}Li_{0.0375})$ $(Nb_{0.9625-x}Sb_xTa_{0.0375})O_3$ (KNLNST) ceramics were prepared by normal sintering and their electrical properties were investigated with a special emphasis on the influence of Sb content.

2. Experimental

K_2CO_3 (99%), Na_2CO_3 (99.8%), Li_2CO_3 (98%), Nb_2O_5 (99.5%), Ta_2O_5 (99.99%), and Sb_2O_3 (99.5%) were used as raw materials to prepare $(K_{0.4425}Na_{0.52}Li_{0.0375})$ $(Nb_{0.9625-x}Sb_xTa_{0.0375})O_3$ ($x = 0.05$, 0.06, 0.07, 0.08, and 0.09) ceramics by

---

* Corresponding author. Tel.: +86 25 84891123; fax: +86 25 84891123.
E-mail address: qiu@nuaa.edu.cn (J. Qiu).

0272-8842/$36.00 © 2011 Elsevier Ltd and Techna Group S.r.l. All rights reserved.
doi:10.1016/j.ceramint.2011.08.056

the conventional mixed-oxide method. The stoichiometric powders were mixed by ball-milling in ethanol for 5 h, then dried and calcined at 900 °C for 5 h. The calcined powders were mixed with 3 wt% polyvinyl alcohol (PVA) solution, and then uniaxially pressed into pellets with a diameter of 1.5 cm under 300 MPa pressure. After burning out PVA, the green disks were respectively sintered in air at selected temperatures for 3 h, depending on x, in the range between 1100 and 1140 °C.

Density of samples was determined by the Archimedes method. The crystal structure was determined using X-ray powder diffraction with a Cu Kα radiation (Bruker D8 Advance, Germany). Raman spectra (Jobin Yvon Labram HR800, France) investigation was performed at room temperature. The microstructure was observed by using a scanning electron microscope (JSM-5610LV/Noran-Vantage). For the measurement of dielectric and piezoelectric properties, silver paste electrodes were formed at the two circular surfaces of the disk-shaped specimens after firing at 700 °C for 10 min. Dielectric properties as a function of temperature and frequency were measured by an impedance analyzer (HP4294A). Polarization versus electric field hysteresis loops were measured using a ferroelectric test system (TF Analyzer 2000). Before measuring the relevant electrical properties, the sintered samples were poled under 30 kV/cm bias at 110 °C in a silicone oil bath for 30 min and then aged at room temperature for 24 h after poling. The piezoelectric constant d_{33} was measured using a quasistatic piezoelectric constant testing meter (ZJ-3A, Institute of Acoustics, Chinese Academy of Science, Beijing, China).

3. Results and discussion

Fig. 1 shows the X-ray diffraction patterns between the 2θ range 20–60° (a) and 30–34° (b) for $(K_{0.4425}Na_{0.52}Li_{0.0375})(Nb_{0.9625-x}Sb_xTa_{0.0375})O_3$ ceramics. All the ceramics are of the single perovskite phase, which indicates that Sb^{5+} seems to have diffused into the perovskite lattice to form a solid solution, in which Sb^{5+} occupies the B-site of the ABO_3 structure. The diffraction peaks slightly shift to a higher angle with increasing Sb content as highlighted in Fig. 1(b), and the inter-planar distance which is deduced by Bragg's equation ($2d \sin \theta = \lambda$) decreases gradually. The slight decrease of inter-planar crystal spacing along to (1 1 1) should be caused by the substitution of a part of Sb^{5+} for Nb^{5+}, since the ionic radius of Sb^{5+} (0.62 Å) is smaller than that of Nb^{5+} (0.69 Å).

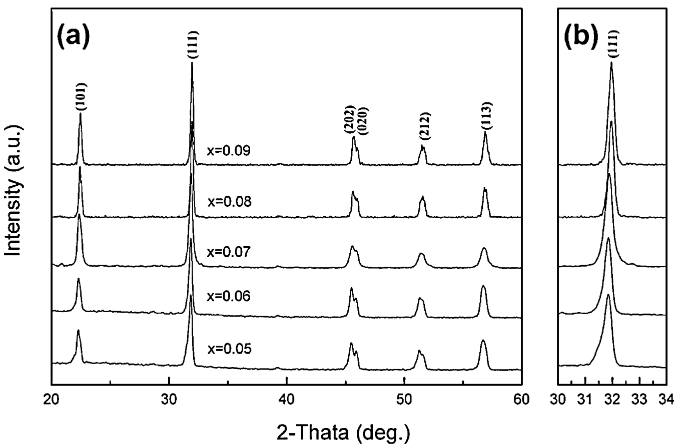

Fig. 1. X-ray diffraction patterns between the 2θ range 20–60° (a) and 30–34° (b) for $(K_{0.4425}Na_{0.52}Li_{0.0375})(Nb_{0.9625-x}Sb_xTa_{0.0375})O_3$ ceramics.

The results of Raman spectrum experiments performed at room temperature for the samples $(K_{0.4425}Na_{0.52}Li_{0.0375})(Nb_{0.9625-x}Sb_xTa_{0.0375})O_3$ ($x = 0.05$, 0.07 and 0.09) are shown in Fig. 2. Three obvious bands can be seen at $x = 0.05$, in a descending order, at 200–350, 500–700, and 800–900 cm^{-1} in the Raman shift range of 200–1000 cm^{-1}. Three bands slightly shift to lower frequency numbers with the increase in Sb concentration, as shown in Fig. 2. We attribute these differences to the anharmonic vibrations because of the disorder in the B sites and distortion of the corner-sharing NbO_6 octahedron clusters caused by Sb partial substitution for Nb. By increasing x, all the bands shift to lower frequency numbers [14]. The much higher Pauling electronegativity of Sb (2.05) compared with Nb (1.60) makes the KNN-based perovskite more covalent [14]; the Sb–O bond has lower bond energy (372 kJ/mol) and weaker polarization than the Nb–O bond (753 kJ/mol) [15]. In addition, because the Sb^{5+} radius is smaller than that of Nb^{5+}, Sb substitution may give rise to a larger off-centering of the cation and induce the distortion of crystal lattice. All the above reasons may result in the fall of the $[BO_6]$ force constant in the lattice and the weakness of the stability of the central ion in the oxygen octahedron, which result in the shifting of the bands to lower wave numbers [16].

Fig. 3 shows the SEM micrographs of the surface for the $(K_{0.4425}Na_{0.52}Li_{0.0375})(Nb_{0.9625-x}Sb_xTa_{0.0375})O_3$ ($x = 0.05$, 0.06, 0.07, 0.08, 0.09) ceramics after sintering. The ceramics with $x = 0.05$ include homogeneous fine grains of 1–2 μm. By increasing x to 0.06, the grain size slightly increases to around 3–4 μm and the microstructure remains relatively uniform. However, the ceramics show the densest microstructures of typical bimodal grain size distributions for the $(K_{0.4425}Na_{0.52}Li_{0.0375})(Nb_{0.8925}Sb_{0.07}Ta_{0.0375})O_3$ ($x = 0.07$) ceramics. The bimodal grain size of ceramics with $x = 0.07$

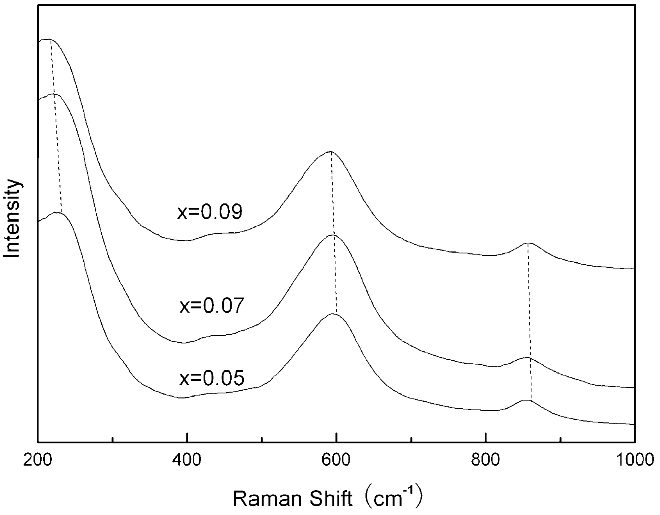

Fig. 2. Raman spectra of the ceramics with different Sb contents.

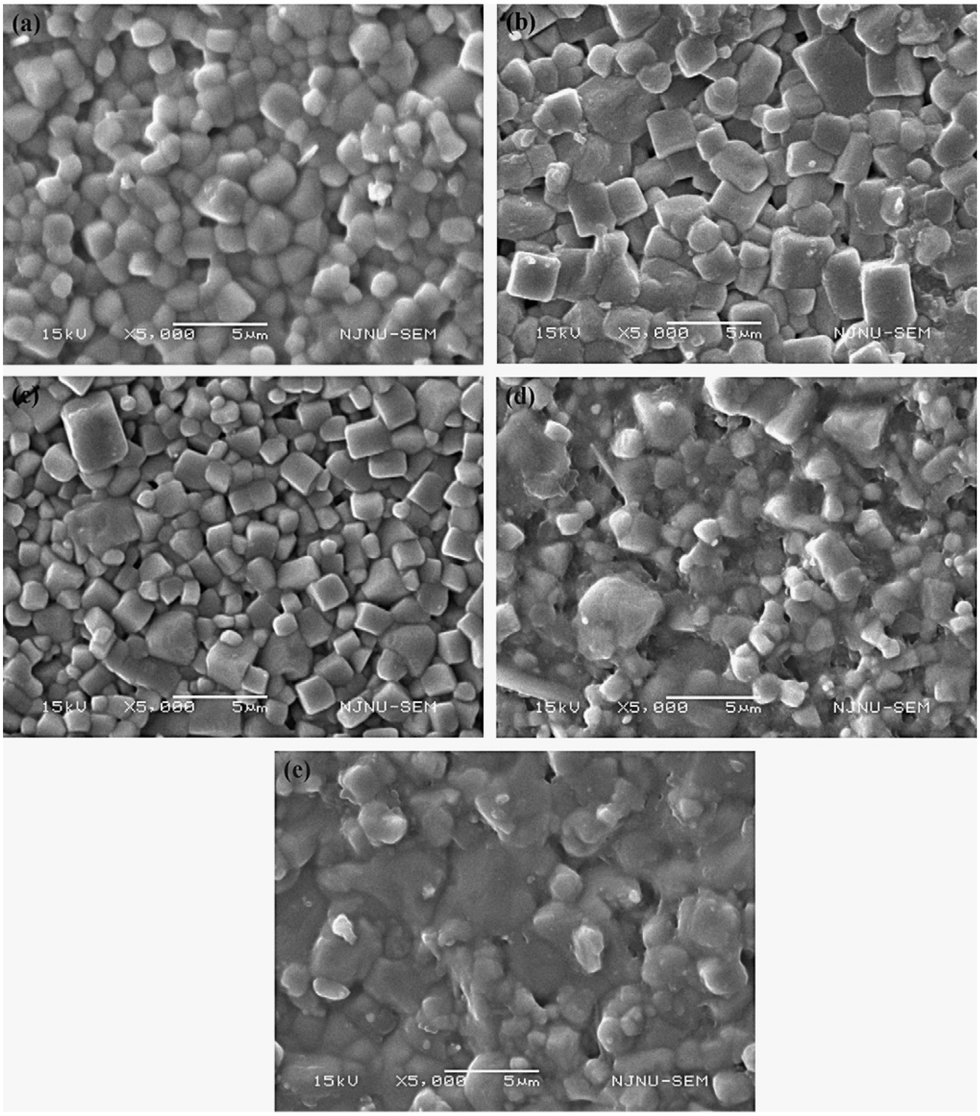

Fig. 3. SEM micrographs of $(K_{0.4425}Na_{0.52}Li_{0.0375})$ $(Nb_{0.9625-x}Sb_xTa_{0.0375})O_3$ ceramics sintered at 1120°C with various Sb contents: (a) $x = 0.05$, (b) $x = 0.06$, (c) $x = 0.07$, (d) $x = 0.08$, and (e) $x = 0.09$.

is about 1 and 4 μm. A molten microstructure with abnormal grains and blur grain boundary can be seen from the ceramics with x from 0.08 to 0.09. The result shows that a well and dense microstructure cannot be obtained for the ceramics with $x > 0.07$.

Fig. 4 shows the piezoelectric coefficient d_{33}, planar mode electromechanical coupling coefficient k_p, dielectric constant ε_r, and dielectric loss tan δ as a function of Sb content for the $(K_{0.4425}Na_{0.52}Li_{0.0375})$ $(Nb_{0.9625-x}Sb_xTa_{0.0375})O_3$ ceramics at room temperature. The ceramics with $x = 0.05$ have the highest k_p (0.52). The slight decreases of k_p can be seen with increasing x to 0.08, and it is 0.46. Further increasing x to 0.09 causes rapid decreases, which is 0.16. Both d_{33} and ε_r curves show almost the same trend for the ceramics. Since all the ceramics show the same orthorhombic symmetry structure and an absent morphotropic phase boundary (Fig. 1), the electrical properties of the piezoelectric ceramics at room temperature are sensitive mainly to the microstructure as wall as density rather than the phase structure. Furthermore, the tan δ firstly shows a slight

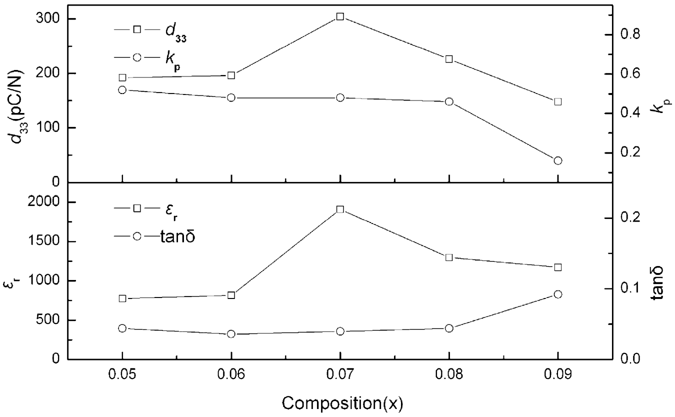

Fig. 4. Dielectric and piezoelectric properties of the ceramics with different Sb contents at room temperature.

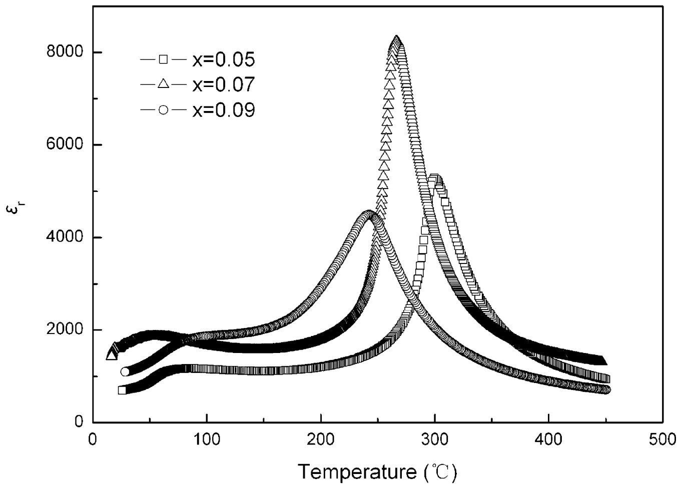

Fig. 5. Temperature dependence of ε_r for the ceramics with different Sb contents (at 1 kHZ).

decrease to 0.036 at $x = 0.06$, then it increases slightly to 0.044 at $x = 0.08$. From then onwards, it rapidly increases to 0.092 at $x = 0.09$. The sample with $x = 0.07$ exhibits excellent properties: high piezoelectric constant of $d_{33} = 304$ pC/N, low dielectric loss of $\tan\delta = 0.04$, high dielectric constant of $\varepsilon_r = 1909$, and high planar and thickness electromechanical coupling coefficients of $k_p = 0.48$, which is well consistent with the microstructure (Fig. 3).

Fig. 5 shows the temperature dependence of the dielectric permittivity for the $(K_{0.4425}Na_{0.52}Li_{0.0375})(Nb_{0.9625-x}Sb_xTa_{0.0375})O_3$ samples of $x = 0.05$, 0.07 and 0.09, which was measured at 1 kHZ. Above room temperature, orthorhombic-structured ceramics such as pure (K, Na)NbO$_3$ ceramics would undergo two-phase transitions from paraelectric cubic to ferroelectric tetragonal at the Curie point ($T_{T\text{–}C}$) and from ferroelectric tetragonal to ferroelectric orthorhombic at the second phase transitional point ($T_{O\text{–}T}$), respectively [17]. High Curie temperatures ($T_C > 241$°C) are obtained in all the KNLNST samples. The samples with $x = 0.05$ and 0.07 undergo two phase transitions from tetragonal polymorphic phase to cubic phase (T_C) at 300 °C, 271 °C, and from orthorhombic to tetragonal polymorphic phase (T_{O-T}) at 85 °C, 50 °C, respectively. With increasing x, both T_C and T_{O-T} shift to lower temperatures. Interestingly, a different variation trend can be observed at $x = 0.09$. The dielectric constant firstly increases, and a "shoulder" occurs at around 90°C, and then it begins to increase rapidly to the maximum value at T_C (241 °C). The different phenomenon observed at $x = 0.09$ may result from the fact that the ceramics at $x = 0.09$ have a distortion of crystal structure, low density, and poor microstructure at room temperature. Furthermore, some broadening of the tetragonal–cubic transition peak can be observed by increasing x, which may imply a relaxor-type phase transition.

A modified empirical expression is proposed by Uchino and Nomura to describe the diffuseness of the ferroelectric phase transition [18],

$$\frac{1}{\varepsilon} - \frac{1}{\varepsilon_m} = \frac{(T - T_m)^r}{C} \tag{1}$$

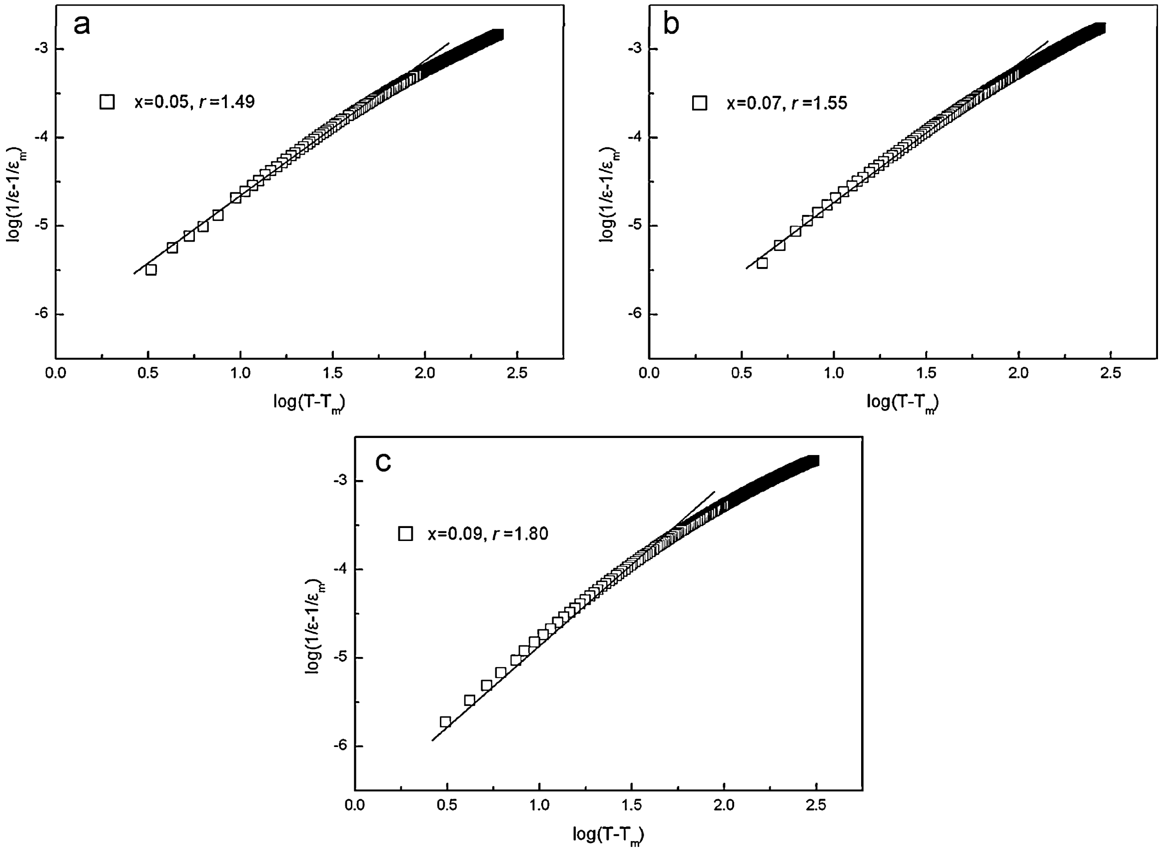

Fig. 6. Log($1/\varepsilon - 1/\varepsilon_m$) as a function of log($T - T_m$) for the $(K_{0.4425}Na_{0.52}Li_{0.0375})(Nb_{0.9625-x}Sb_xTa_{0.0375})O_3$ ceramics with various Sb contents.

where ε_m is the peak value of the dielectric constant and T_m is the temperature at which the ε value reaches the maximum. r and C are assumed to be constant; the r value is between 1 and 2. The limiting value $r = 1$ makes the equation fit the conventional Curie–Weiss law valid for the normal ferroelectric, and $r = 2$ makes the equation fit the quadratic valid for an ideal relaxor ferroelectric. When r is between 1 and 2, it indicates a so-called incomplete diffuse phase transition. Based on the temperature plots of ε_r, the graph of $\log(1/\varepsilon - 1/\varepsilon_m)$ versus $\log(T - T_m)$ for the ceramics is plotted and the results are shown in Fig. 6(a)–(c). The slope of the fitting curves is used to determine the r values. The r values are 1.49, 1.56 and 1.89 at $x = 0.05$, 0.07 and 0.09 respectively, which indicates that these ceramics, especially the $(K_{0.4425}Na_{0.52}Li_{0.0375})(Nb_{0.9625-x}Sb_xTa_{0.0375})O_3$ samples of $x = 0.09$ show an intermediate relaxor-like behavior between normal and ideal relaxor ferroelectrics due to both the A-site cation mixtures and B-site cation mixtures.

Fig. 7 shows the dielectric constant as a function of the temperature for the ceramics with $x = 0.09$ under different measuring frequencies. The value of ε_r decreases with increasing the measuring frequency. A small amount of the frequency dispersion of ε_r values exists between 100 Hz and 100 kHz, which present T_m of 239, 241, 242, and 243 °C. It has been known that for the A-site complex $(A_1A_2)BO_3$ and B-site complex $A(B_1B_2)O_3$ perovskite ferroelectrics, a small difference in ionic radii of the A- or B-site cations is favorable for the formation of a disordered structure [19]. As there is a small difference of the ionic radii between Nb^{5+} and Sb^{5+}, the substitution of Sb^{5+} for Nb^{5+} increases the B-site disordered degree and hence the local compositional fluctuation. As a result, the ceramics become more relaxor.

The polarization-electric field hysteresis loops for KNLNST ceramics are presented in Fig. 8. As shown in Fig. 8, the ceramics with $x = 0.05$ possess a large remnant polarization ($P_r = 20.7\ \mu C/cm^2$) and coercive field ($E_c = 9.1$ kV/cm), but low piezoelectric performance for the poor microstructure and densification is also observed from Figs. 3 and 4. It should be noted that the remnant polarization decreases by 6% but the coercive field decreases by 11% when $x = 0.07$($P_r = 19.4\ \mu C/cm^2$, $E_c = 8.1$ kV/cm). The results indicate that the ceramics with $x = 0.07$ exhibit higher piezoelectric activity. Comparing with the KNLNST ceramics with $x = 0.05$, the coercive field decreases by 11% while the remnant polarization of the ceramics with $x = 0.07$ just slightly decreases. The piezoelectric activity is higher for the KNLNST ($x = 0.07$) ceramics because the lower the coercive field can improve the domain reorientation. Further increasing x to 0.09 causes the rapid decrease of both P_r and E_c, and unsaturated hysteresis loop is observed. It suggests that a well-saturated P–E loop can be obtained for the ceramics with $x = 0.07$.

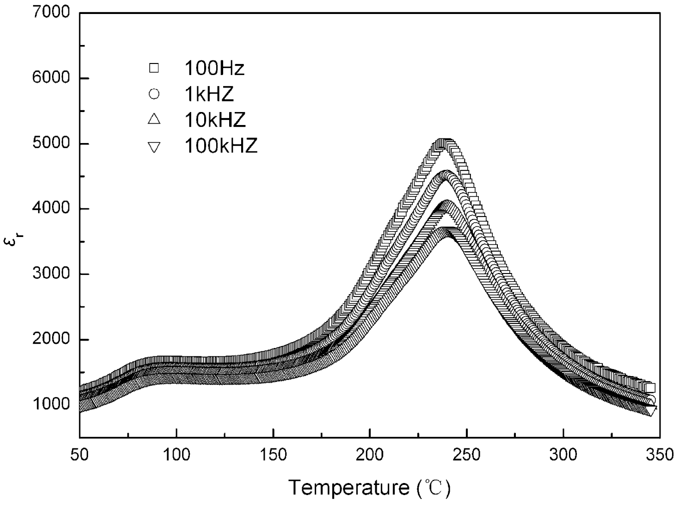

Fig. 7. The dielectric constant as a function of the temperature for $(K_{0.4425}Na_{0.52}Li_{0.0375})(Nb_{0.9625-x}Sb_xTa_{0.0375})O_3$ ceramics of $x = 0.09$.

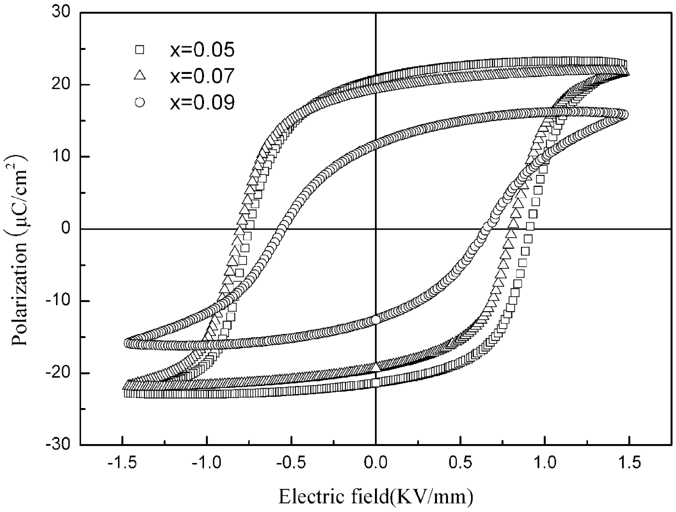

Fig. 8. P–E hysteresis loops of the ceramics with different Sb contents.

4. Conclusions

The effects of the Sb content on the phase structure, microstructure, dielectric, piezoelectric, and ferroelectric properties of the $(K_{0.4425}Na_{0.52}Li_{0.0375})(Nb_{0.9625-x}Sb_xTa_{0.0375})O_3$ ceramics were investigated. The results of the X-ray diffraction patterns show that a single perovskite structure were obtained by the whole compositional samples, and all the bands in the Raman spectra shift to lower frequency numbers. However, owing to the densest microstructure of typical bimodal grain size distributions, the $(K_{0.4425}Na_{0.52}Li_{0.0375})(Nb_{0.8925}Sb_{0.07}Ta_{0.0375})O_3$ ceramic shows optimum electrical properties, such as piezoelectric coefficient (d_{33}), electromechanical coupling coefficient (k_p), and dielectric constant (ε), which are 304 pC/N, 48%, and 1909, respectively. The tetragonal–cubic phase transition can be observed from all the ceramics above room temperature in the $\varepsilon_r - T$ curves. The orthorhombic–tetragonal phase transition can be shifted from about 85 °C to lower temperature by increasing x. By increasing x from 0 to 0.09, the P_r and E_c values decrease.

Acknowledgements

This work was supported by the National Nature Science Foundation of China (NSFC No. 90923029, 50830201), the Natural Science Foundation of Jiangsu Province of China (BK2009020), Program for Changjiang Scholars and Innovative Research Team in University (IRT0968), Program for New Century Excellent Talents in University (NCET-10-0070), A Project Funded by the Priority Academic Program Development of Jiangsu Higher Education Institutions, and NUAA Research Fund for Fundamental Research (NJ2010010, NZ2010001).

References

[1] Y. Saito, H. Takao, T. Tani, T. Nonoyama, K. Takatori, T. Homma, T. Nagaya, M. Nakamura, Lead-free piezoceramics, Nature 432 (2004) 84–87.

[2] I.H. Chan, C.T. Sun, M.P. Houng, S.Y. Chu, Sb doping effects on the piezoelectric and ferroelectric characteristics of lead-free $Na_{0.5}K_{0.5}Nb_{1-x}Sb_xO_3$ piezoelectric ceramics, Ceram. Int. 37 (2011) 2061–2068.

[3] J.F. Li, K. Wang, B.P. Zhang, L.M. Zhang, Ferroelectric, Piezoelectric properties of fine-grained $Na_{0.5}K_{0.5}NbO_3$ lead-free piezoelectric ceramics prepared by spark plasma sintering, J. Am. Ceram. Soc. 89 (2006) 706–709.

[4] R.Z. Zuo, J. Rodel, R.Z. Chen, L.T. Li, Sintering, Electrical properties of lead-free $Na_{0.5}K_{0.5}NbO_3$ piezoelectric ceramics, J. Am. Ceram. Soc. 89 (2006) 2010–2105.

[5] H.L. Du, Z.M. Li, F.S. Tang, S.B. Qu, Z.B. Pei, W.C. Zhou, Preparation and piezoelectric properties of lead-free piezoelectric ceramics with pressure-less sintering, Mater. Sci. Eng. B. 131 (2006) 83–87.

[6] B. Malic, D. Jenko, J. Holc, M. Hrovat, M. Kosec, Synthesis of sodium potassium niobate: a diffusion couples study, J. Am. Ceram. Soc. 91 (2008) 1916–1922.

[7] R.E. Jaeger, L. Egerton, Hot pressing of potassium-sodium niobates, J. Am. Ceram. Soc. 45 (1962) 209–213.

[8] B.P. Zhang, J.F. Li, K. Wang, H.L. Zhang, Compositional dependence of piezoelectric properties in $Na_xK_{1-x}NbO_3$ lead-free ceramics prepared by spark plasma sintering, J. Am. Ceram. Soc. 89 (2006) 605–1609.

[9] W. Yang, D.R. Jin, T.T. Wang, J.R. Cheng, Effect of oxide dopants on the structure and electrical properties of $(Na_{0.5}K_{0.5})NbO_3$–$LiSbO_3$ lead-free piezoelectric ceramics, Physica B 405 (2010) 1918–1921.

[10] S.J. Zhang, R. Xia, T.R. Shrout, G.Z. Zang, J.F. Wang, Characterization of lead free $(K_{0.5}Na_{0.5})$ NbO_3–$LiSbO_3$ piezoceramic, Solid State Commun. 141 (2007) 675–679.

[11] Y.H. Zhen, J.F. Li, Normal sintering of (K, Na) NbO_3-based ceramics: influence of sintering temperature on densification, microstructure, and electrical properties, J. Am. Ceram. Soc. 89 (2006) 3669–3675.

[12] H. Takao, Y. Saito, Y. Aoki, K. Horibuchi, Microstructural evolution of crystalline-oriented $(K_{0.5}Na_{0.5})$ NbO_3 piezoelectric ceramics with a sintering aid of CuO, J. Am. Ceram. Soc. 89 (2006) 951–1956.

[13] H.D. Li, W.Y. Shih, W.H. Shih, Effect of antimony concentration on the crystalline structure, dielectric, and piezoelectric properties of $(Na_{0.5}K_{0.5})_{0.945}$ $Li_{0.055}Nb_{1-x}Sb_xO_3$ solid solutions, J. Am. Ceram. Soc. 90 (2007) 3070–3072.

[14] L.K. Su, K.J. Zhu, L. Bai, J.H. Qiu, H.L. Ji, Effects of Sb-doping on the formation of (K, Na) (Nb, Sb)O_3 solid solution under hydrothermal conditions, J. Alloy Compd. 493 (2010) 186–191.

[15] Y.F. Chang, Z.P. Yang, L.R. Xiong, Z.H. Liu, Z.L. Wang, Phase structure, microstructure, and electrical properties of Sb-modified (K, Na, Li) (Nb, Ta)O_3 piezoelectric ceramics, J. Am. Ceram. Soc. 91 (2008) 2211–2216.

[16] M.K. Zhu, P.X. Lu, Y.D. Hou, X.M. Song, H. Wang, H. Yan, Analysis of phase coexistence in Fe_2O_3-doped 0.2PZN–0.8PZT ferroelectric ceramics by Raman scattering spectra, J. Am. Ceram. Soc. 89 (2006) 3739–3744.

[17] Y.F. Chang, Z.P. Yang, X.L. Chao, R. Zhang, X.R. Li, Dielectric and piezoelectric properties of alkaline-earth titanate doped $(K_{0.5}Na_{0.5})NbO_3$ ceramics, Mater. Lett. 61 (2007) 785–789.

[18] K. Uchino, S. Nomura, Critical exponents of the dielectric constants in diffused phase transition crystals, Ferroelectr. Lett. Sect. 44 (1982) 55–56.

[19] D.M. Lin, K.W. Kwok, H.L.W. Chan, Microstructure, phase transition, and electrical properties of $(K_{0.5}Na_{0.5})_{1-x}Li_x$ $(Nb_{1-y}Ta_y)O_3$ lead-free piezoelectric ceramics, J. Appl. Phys. 102 (2007), 034102-1–034102-7.